JACS
JOURNAL OF THE AMERICAN CHEMICAL SOCIETY
pubs.acs.org/JACS
Article

Solvent Polarity Effects on the Mechanochemistry of Spiropyran Ring Opening

Yangju Lin, Tatiana B. Kouznetsova, Alex G. Foret, and Stephen L. Craig*

Cite This: *J. Am. Chem. Soc.* 2024, 146, 3920−3925

Read Online

ACCESS | Metrics & More | Article Recommendations | Supporting Information

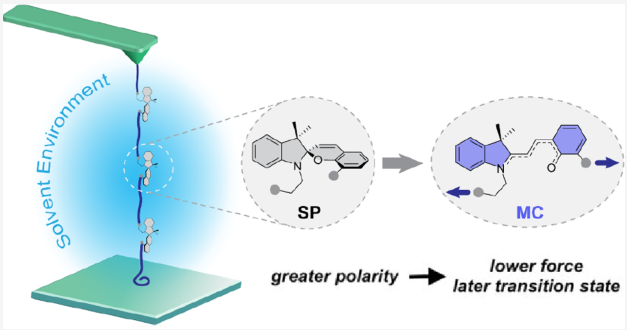

ABSTRACT: The spiropyran mechanophore (SP) is employed as a reporter of molecular tension in a wide range of polymer matrices, but the influence of surrounding environment on the force-coupled kinetics of its ring opening has not been quantified. Here, we report single-molecule force spectroscopy studies of SP ring opening in five solvents that span normalized Reichardt solvent polarity factors (E_T^N) of 0.1−0.59. Individual multimechanophore polymers were activated under increasing tension at constant 300 nm s^{-1} displacement in an atomic force microscope. The extension results in a plateau in the force−extension curve, whose midpoint occurs at a transition force f^* that corresponds to the force required to increase the rate constant of SP activation to approximately 30 s^{-1}. More polar solvents lead to mechanochemical reactions that are easier to trigger; f^* decreases across the series of solvents, from a high of 415 ± 13 pN in toluene to a low of 234 ± 9 pN in *n*-butanol. The trend in mechanochemical reactivity is consistent with the developing zwitterionic character on going from SP to the ring-opened merocyanine product. The force dependence of the rate constant ($\Delta x^\ddagger$) was calculated for all solvent cases and found to increase with E_T^N, which is interpreted to reflect a shift in the transition state to a later and more productlike position. The inferred shift in the transition state position is consistent with a double-well (two-step) reaction potential energy surface, in which the second step is rate determining, and the intermediate is more polar than the product.

■ INTRODUCTION

When a polymer network is subjected to externally applied stress and strain, the molecular strands within it experience tension. The tension is unevenly distributed at the molecular level, and individual strands may experience forces that are large enough to overstretch and even cleave covalent bonds. These bond stretching[1−4] and scissile[5,6] physical properties of strands are tied to the chemical composition of the polymer, and they are implicated in the high strain behavior and degradation of polymeric materials.[7,8] Insights into the molecular responses that accompany macroscopic mechanical behavior can be obtained by embedding mechanophores[9] that generate a constructive response to high forces of tension. Mechanically triggered signals that report stress or damage[10] are particularly useful. The capability to report stress or damage is realized through insertion of force probes, typically mechanochromic probes, and the corresponding mechanochromism can be utilized to visualize forces in the materials.[10−12]

Reported mechanochromic probes include spiropyran (SP),[13,14] dioxetanes,[15] and rhodamine,[16,17] among others. SP force probes have received considerable attention owing to their accessible synthesis,[18] the high extinction coefficient of the merocyanine (MC) product of their mechanically coupled ring-opening reaction (Figure 1), and the ability to tune their mechanochemical activity though regiochemistry or substituents.[13,14,19]

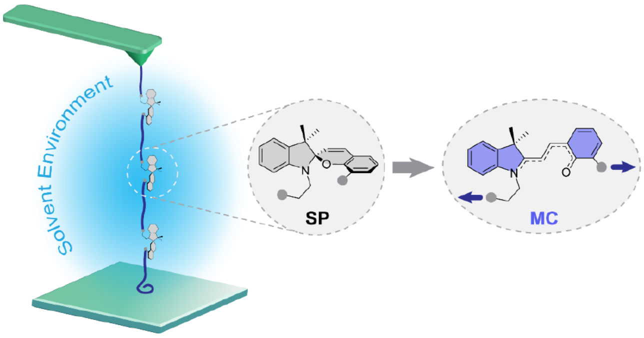

Figure 1. Schematic representation of single molecule force spectroscopy (SMFS) of spiropyran mechanophore opening to the merocyanine form as a function of solvent environment.

SP probes have been explored in a range of polymer matrices, including polyacrylates,[13] polycaprolactone,[12,20] polycarbon-

Received: October 18, 2023
Revised: January 23, 2024
Accepted: January 24, 2024
Published: February 3, 2024

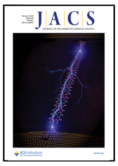

https://doi.org/10.1021/jacs.3c11621
J. Am. Chem. Soc. 2024, 146, 3920−3925

ate,[21] poly(ionic liquid),[22] acrylic latex,[23] polystyrene,[24] polyurethanes,[25] polyphenylenes,[26] and hydrogels.[27−29] SP mechanochromism has revealed contributions of mobility,[30] relaxation,[31−33] and alignment[34−37] of polymer chains to molecular-level force transduction. Underlying these responses is the actual force required for SP activation, which is sometimes considered explicitly.[26,38,39] Quantitative interpretation is facilitated by a handful of experimental[14,40] and computational[41−43] studies of force-coupled SP reaction kinetics.

An important knowledge gap remains, however. The range of materials investigated spans a range of dielectric constants and protic/aprotic character, and whereas the effect of chemical environment (solvent[44]) or polymer matrix[45] on SP/MC equilibria has been reported, the corresponding influence on SP mechanochemistry has yet to be determined.[46] We, therefore, sought to quantify the mechanochemical kinetics of a model SP ring opening in solvents of various polarities (E_T^N), providing an entry into the largely unexplored topic of solvent effects on mechanochemical reactions[47,48] that complements other quantitative structure−activity relationships.[14,49−57]

Our approach comprises probing mechanically coupled SP-to-MC kinetics via the single-molecule force spectroscopy (SMFS) of multimechanophore polymers,[58] a technique that has been extensively applied previously.[59] The use of multimechanophore polymers means that a single successful pull provides hundreds of reactions and thus good statistics for analysis. As illustrated in Figure 1, a polymer bearing multiple SPs is trapped between the cantilever of an atomic force microscope and a substrate, which separates to extend the polymer chain and accelerate the SP ring opening. Rates are obtained by fitting the force curves. Here, we employ an SMFS in a range of solvents to quantify solvent effects on the mechanochemical reaction.

■ RESULTS

We prepared a copolymer comprising 44 mol % SP and 56 mol % 9-oxabicyclo[6.1.0]non-4-ene (epoxy-COD) repeats along the polymer backbone using methods based on entropy-driven ring opening metathesis polymerization[60] (Figure 2a). The epoxy-COD comonomer enhances polymer adhesion to the substrate and cantilever during the approach-retraction cycles, in which the epoxide presumably allows for covalent bonding between the polymer chain and surface.[61] We sought to further improve the reactivity of the bonding reaction using an amine-functionalized silicon substrate (see Supporting Information). Solvents were chosen based on desirable criteria: low viscosity, high boiling point, and a wide range of relative polarity. These criteria resulted in the use of toluene, methyl benzoate (MB), pyridine, dimethyl formaldehyde (DMF), and *n*-butanol (relevant parameters are listed in Table S1).

SMFS studies were performed using an approach/retraction cycle at a vertical displacement velocity of 300 nm/s, and Figure 2b shows a representative set of normalized force−extension curves obtained in a series of solvents. The characteristic plateaus originate from the mechanically induced SP-to-MC transformation, as MC is more extended than SP, and the resulting extra extension (L_f/L_i) agrees with computed values (see Supporting Information). An increase in solvent polarity (E_T^N) leads to a shift in the plateau force, which decreases from 415 ± 13 pN in toluene to 234 ± 9 pN in *n*-butanol. Notably, the relative length of transitions observed in these solvents is almost identical, indicating that the plateau corresponds to the mechanochemically triggered SP-to-MC transformation and ruling out solvent-induced entropic change associated with polymer conformation,[62] consistent with previous observations.[63,64]

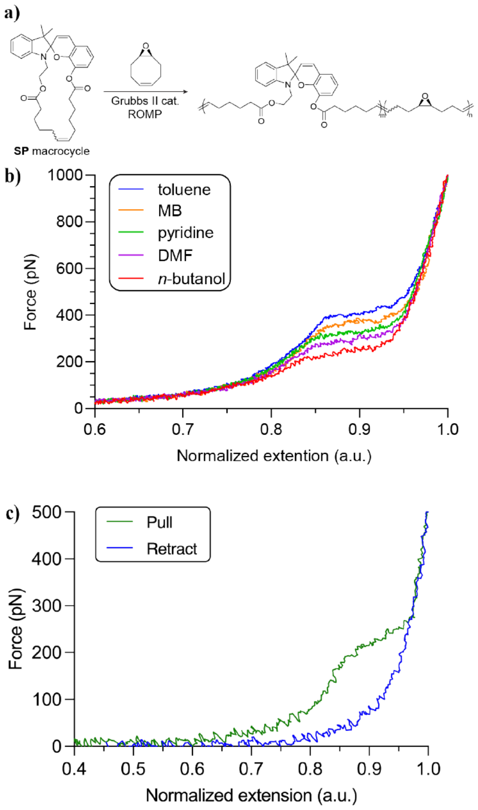

Figure 2. a) Synthetic scheme of a copolymer containing multiple SPs (44 mol %) along the backbone. b) Overlay of representative force−extension curves obtained in various solvents. The SMFS was performed at a constant retraction rate of 300 nm/s, and the curves are normalized to the corresponding extension at 1 nN force. c) SMFS curve of the polymer in *n*-butanol during loading (green) and immediate unloading (blue).

Prior SMFS studies in toluene − the least polar solvent employed in this study − have demonstrated that the rate of the reverse MC-to-SP reaction is slow relative to the time scale of the SMFS experiment.[14] In other words, the observed plateau is under kinetic, rather than thermodynamic, control. Because the barrier for the reverse reaction increases with solvent polarity,[65] we expected that the kinetic control would extend to the polar end of the solvent spectrum employed. That expectation was confirmed by the observation of hysteresis in the loading−unloading SMFS curve of a single polymer chain in *n*-butanol (Figure 2c). The observed hysteresis rules out the possibility that the plateau is reflecting a force-coupled equilibrium, and the transition forces observed, therefore, reflect the relative force-coupled kinetics of the ring-opening reaction at both ends of the solvent polarity spectrum investigated.

Transition force was plotted against relative solvent polarity (E_T^N), where E_T^N is defined as E_T[30] of a given solvent normalized to that of water (Figure 3a). We chose E_T^N because of its prior association with the kinetics of SP ring opening,[66−68] and it shows the best correlation out of multiple solvent parameters considered (see Supporting Information). The plot shows a strong linear correlation across the range of solvents investigated. In more polar solvents, the reaction requires less force to reach rates of reactive extension that are competitive

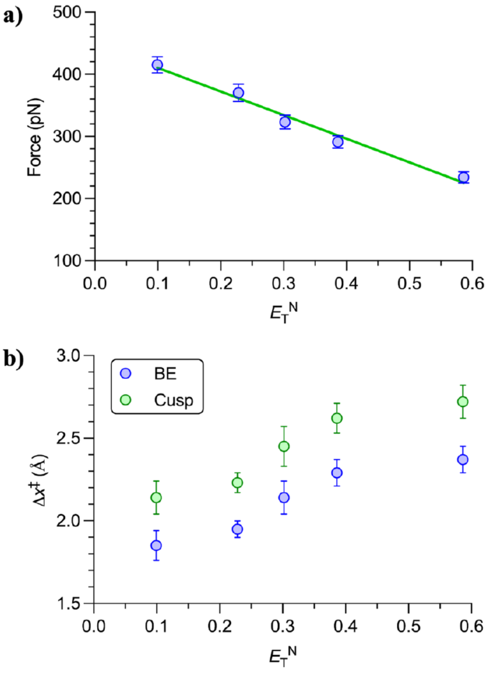

Figure 3. a) Observed transition forces in SMFS experiments as a function of solvent polarity (E_T^N), with the best linear fit shown ($y = -379x + 448$, $R^2 = 0.982$); b) Mechanochemical coupling parameter vs solvent polarity (E_T^N).

with the rate of SMFS tip−surface displacement. This correlation is consistent with a reaction that is intrinsically more facile in a polar environment. The force-free SP-to-MC conversion proceeds through an intermediate that is more polar than the reactant, and whose zwitterionic character increases with E_T^N.[66−68] A similar change in polarity has been inferred in the mechanochemical reaction.[14] Prior computations suggest that developing charge separation during initial C−O bond dissociation leads to a lower activation energy with increasing E_T^N.[65,69] Figure 3a indicates that this trend applies to the SP mechanochemical reactivity as well.

The SMFS curves were further analyzed by fitting them to two classic, empirical models of mechanochemical kinetics: the Eyring model popularized by Bell and Evans (eq 1),[70] and the so-called cusp model developed by Dudko, Hammer, and Szabo (eq 2).[71] The force-free rate constant k_0 and activation energy $\Delta G^{\ddagger}$ were obtained and extrapolated from reported values (Figure S1), and the two models were fit to the SMFS data by varying the mechanical coupling parameter $\Delta x^{\ddagger}$, which within the assumptions of the models corresponds to the difference in end-to-end distance between ground and transition states that is coupled to the tension applied to the reaction.

$$k(F) = k_0\, e^{F\Delta x^{\ddagger}/k_BT} \tag{1}$$

$$k(F) = k_0\left(1 - \frac{F\Delta x^{\ddagger}}{2\Delta G^{\ddagger}}\right) e^{F\Delta x^{\ddagger}/k_BT - (F\Delta x^{\ddagger})^2/4\Delta G^{\ddagger}k_BT} \tag{2}$$

The resulting values of $\Delta x^{\ddagger}$ are shown in Figure 3b. The accuracy and precision of the absolute values of the extracted $\Delta x^{\ddagger}$ in terms of a specific molecular dimension are uncertain, in particular because the low forces of the SP-to-MC transition relative to other covalent mechanophores mean that the reacting polymer in the present study is not as conformationally constrained as in SMFS studies of other mechanophores. Nonetheless, given that the same polymer, SMFS method, and analysis methods are used across the series, the trend in $\Delta x^{\ddagger}$ is likely to be informative. As seen in Figure 3, the effect of force on the rate, captured by the empirical $\Delta x^{\ddagger}$, increases with increasing E_T^N. A larger $\Delta x^{\ddagger}$ suggests that the transition state of the rate-determining step of the reaction occurs later along the reaction coordinate. In other words, the data suggest that increasing E_T^N simultaneously lowers the overall endothermicity of the reaction, lowers the reaction activation energy, and shifts the position of the transition state later on the reaction path (i.e., makes the transition state more productlike).

The computed mechanism of SP ring opening involves two steps, as shown for the likely predominant MC isomer product TTC (for *trans*/*trans*/*cis*, reflecting the stereochemistry across the three carbon−carbon bonds in the center of the MC structure) in Figure 4. Two aspects of the mechanism are germane. First, the second step is rate determining; TS2 is approximately 10 kcal mol^{-1} higher in energy than TS1.[65] Second, the intermediate TCC formed from initial C−O bond

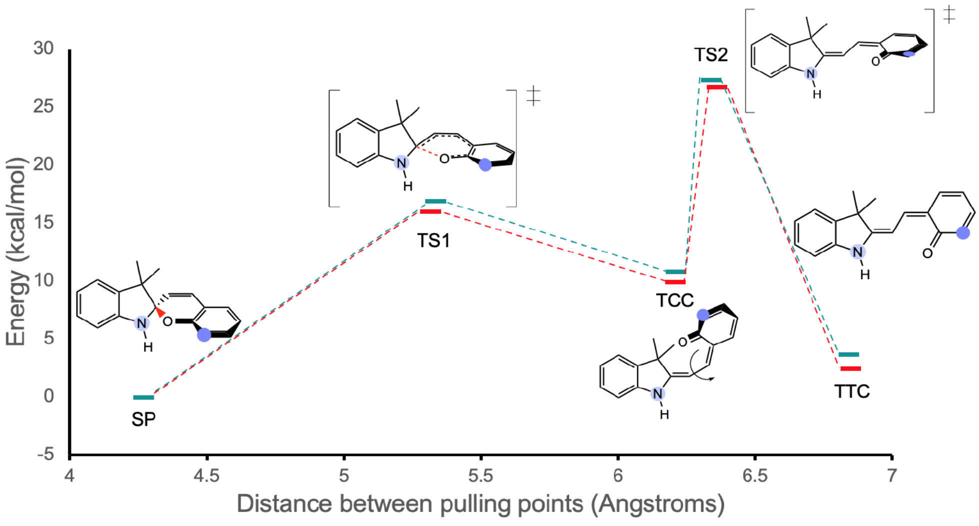

Figure 4. Calculated (DFT B3LYP/6-31G(d)) reaction coordinates in polar (red) and nonpolar (teal) solvents. Distances reported are those between atoms denoted in blue. TTC is the most likely form of the product under mechanical force.[65]

https://doi.org/10.1021/jacs.3c11621

scission is calculated to have a larger dipole moment than TS2 and the ultimate product TTC.[65] Thus, increasing the solvent polarity makes the overall reaction less endothermic, but it also makes the second elementary step in the reaction less exothermic. As a result, traditional qualitative models of reaction surfaces (Hammond's postulate, Marcus theory, etc.) predict that increasing solvent polarity will lead to a later transition state in the second step and, therefore, a later rate determining transition state for the overall reaction, as implied by the greater $\Delta x^‡$. DFT calculations agree well with this model of force-coupled reactivity.

■ DISCUSSION

The relationship between SMFS plateau force and E_T^N described in Figure 3a is different from but related to classical linear free energy relationships. In this case, a mathematical derivation provided in the Supporting Information suggests that the linear relationship of Figure 3a might reasonably be expected, given the successful prior use of E_T^N in linear free energy-type relationships.[72] Given the connection between the two, we emphasize that relationships of this flavor are by their nature, empirical. They quantify the strength of the correlation between two thermodynamic quantities. As such, we do not presume the universality of E_T^N as a stand-alone predictor of all SP mechanochemistry in any solvent or medium, and its validity beyond the solvents examined should not be assumed.

Nonetheless, the correlation of f^* and E_T^N is perhaps not surprising. The origin of E_T^N lies in the molar transition energy associated with the $\pi-\pi^*$ absorption of pyridiniophenolate,[72] and the underlying physical interactions correspond to differential solvation of the excited state (more charge separation) and ground state (less charge separation). There is likewise an increase in charge separation as the SP-to-MC reaction progresses, and the correlation of the associated reaction kinetics and E_T^N has been noted previously. As noted above (and shown in the Supporting Information), the empirical correlation of f^* with E_T^N is better than that with other common solvent parameters. Still, the solvent-induced change in reference electronic absorption energetics is obviously not strictly identical with the solvent-induced change to SP-to-MC reactivity, and so one should remain mindful of the limits of this approach.

We were also struck by the interrelationship of solvent effects and mechanochemical coupling, namely, the fact that solvents that enhance reactivity also enhance mechanical susceptibility. On the surface, the constructive reinforcement of the two structure−reactivity effects might appear to contradict intuitive, empirical models of reactivity such as the Bema Hapothle interrelationships.[73] The apparent disconnection arises from the fact that fundamental reactivity concepts of this type are derived in the context of single elementary reaction steps. In contrast, the origin of the behavior here is well understood by the two-step reaction mechanism shown in Figure 4, in which there is a net increase in polarity on going from the reactant to transition state, but the change in polarity is not monotonic. Rather, there is a large increase in polarity in the first step of the reaction (SP to TCC intermediate) and then a smaller decrease in polarity during the second rate-determining step (TCC to TTC). In this analysis, it is important to be mindful of the fact that the second step of the reaction is rate determining, even though the activation energy of the second step is smaller than that of the first step, due to the reversibility of the first and its associated pre-equilibrium. The connection highlights continuing opportunities to connect covalent polymer mechanochemistry and classic physical organic principles of reactivity.[74]

■ CONCLUSION

Single-molecule force spectroscopy provides the force-coupled kinetics of the spiropyran mechanophore reactivity. The inferred solvent effect on mechanical susceptibility is qualitatively consistent with computed potential energy surfaces and with longstanding fundamental structure−activity concepts applied in the context of a multistep reaction. Within the caveats associated with any empirical relationship derived from a finite set of data, the relationships in Figure 3 provide a basis for estimating the forces involved for SP ring opening in a range of solvents or other continuum environments, including gels and bulk polymers, as long as E_T^N is known. We note with interest that a linear relationship between λ_{max} of merocyanine and E_T^N has been reported,[44] meaning that the in situ absorbance spectrum of the activated MC could in principle be used to ascertain the relevant polarity of a given system, which could then be used to determine the force required for activation. Some circumspection is always warranted when extrapolating beyond an available data set, but it is worth noting that the linear fit in Figure 3a leads to an expected transition force of 68 pN in water (E_T^N = 1), which provides a foundation for interpreting future studies of SP mechanochemistry in hydrogels.

■ ASSOCIATED CONTENT

SI Supporting Information

The Supporting Information is available free of charge at https://pubs.acs.org/doi/10.1021/jacs.3c11621.

Polymer synthesis, SMFS experimental procedures, analysis of SMFS curves and additional SMFS curves, DFT calculation, and SMFS retracing results (PDF)

■ AUTHOR INFORMATION

Corresponding Author

Stephen L. Craig − *Department of Chemistry, Duke University, Durham, North Carolina 27708, United States*; orcid.org/0000-0002-8810-0369; Email: stephen.craig@duke.edu

Authors

Yangju Lin − *Department of Chemistry, Duke University, Durham, North Carolina 27708, United States*; orcid.org/0000-0001-6378-7179
Tatiana B. Kouznetsova − *Department of Chemistry, Duke University, Durham, North Carolina 27708, United States*
Alex G. Foret − *Department of Chemistry, Duke University, Durham, North Carolina 27708, United States*; orcid.org/0009-0006-7586-8180

Complete contact information is available at: https://pubs.acs.org/10.1021/jacs.3c11621

Funding

This work was supported by the National Science Foundation under grant CHE-2304884 (S.L.C.).

Notes

The authors declare no competing financial interest.

■ ABBREVIATIONS

SP, spiropyran; MC, merocyanine; SMFS, single molecule force spectroscopy; COD, cyclooctadiene

REFERENCES

(1) Li, T.; Dufresne, E. R.; Kröger, M.; Heyden, S. Siloxane Molecules: Nonlinear Elastic Behavior and Fracture Characteristics. *Macromolecules* **2023**, *56*, 1303−1310.

(2) Lu, S.; Cai, W.; Cao, N.; Qian, H.-J.; Lu, Z.-Y.; Cui, S. Understanding the Extraordinary Flexibility of Polydimethylsiloxane through Single-Molecule Mechanics. *ACS Mater. Lett.* **2022**, *4*, 329−335.

(3) Dai, Y.; Zhang, Z.; Daniels, M.; Bao, Y.; Guan, J.; Zhang, S.; Zhou, R.; Tan, Y.; Liu, L.; Xiao, H.; Cui, S.; Xu, H. Polytelluoxane: A Chalcogen Polymer That Bridges the Gap between Inorganic Oxides and Macromolecules. *Chem.* **2023**, *9*, 2006−2015.

(4) Wakefield, H. T.; Kevlishvili, I.; Wentz, K. E.; Yao, Y.; Kouznetsova, T. B.; Melvin, S. J.; Ambrosius, E. G.; Herzog-Arbeitman, A.; Siegler, M. A.; Johnson, J. A.; Craig, S. L.; Kulik, H. J.; Klausen, R. S. Synthesis and Ring-Opening Metathesis Polymerization of a Strained Trans-Silacycloheptene and Single-Molecule Mechanics of Its Polymer. *J. Am. Chem. Soc.* **2023**, *145*, 10187−10196.

(5) Wang, S.; Beech, H. K.; Bowser, B. H.; Kouznetsova, T. B.; Olsen, B. D.; Rubinstein, M.; Craig, S. L. Mechanism Dictates Mechanics: A Molecular Substituent Effect in the Macroscopic Fracture of a Covalent Polymer Network. *J. Am. Chem. Soc.* **2021**, *143*, 3714−3718.

(6) Lee, B.; Niu, Z.; Wang, J.; Slebodnick, C.; Craig, S. L. Relative Mechanical Strengths of Weak Bonds in Sonochemical Polymer Mechanochemistry. *J. Am. Chem. Soc.* **2015**, *137*, 10826−10832.

(7) Lin, Y.; Kouznetsova, T. B.; Chang, C.-C.; Craig, S. L. Enhanced Polymer Mechanical Degradation through Mechanochemically Unveiled Lactonization. *Nat. Commun.* **2020**, *11*, 4987.

(8) Caruso, M. M.; Davis, D. A.; Shen, Q.; Odom, S. A.; Sottos, N. R.; White, S. R.; Moore, J. S. Mechanically-Induced Chemical Changes in Polymeric Materials. *Chem. Rev.* **2009**, *109*, 5755−5798.

(9) Li, J.; Nagamani, C.; Moore, J. S. Polymer Mechanochemistry: From Destructive to Productive. *Acc. Chem. Res.* **2015**, *48*, 2181−2190.

(10) Imato, K.; Kanehara, T.; Ohishi, T.; Nishihara, M.; Yajima, H.; Ito, M.; Takahara, A.; Otsuka, H. Mechanochromic Dynamic Covalent Elastomers: Quantitative Stress Evaluation and Autonomous Recovery. *ACS Macro Lett.* **2015**, *4*, 1307−1311.

(11) Ducrot, E.; Chen, Y.; Bulters, M.; Sijbesma, R. P.; Creton, C. Toughening Elastomers with Sacrificial Bonds and Watching Them Break. *Science* **2014**, *344*, 186−189.

(12) O'Bryan, G.; Wong, B. M.; McElhanon, J. R. Stress Sensing in Polycaprolactone Films Via an Embedded Photochromic Compound. *ACS Appl. Mater. Interfaces* **2010**, *2*, 1594−1600.

(13) Davis, D. A.; Hamilton, A.; Yang, J.; Cremar, L. D.; Van Gough, D.; Potisek, S. L.; Ong, M. T.; Braun, P. V.; Martínez, T. J.; White, S. R.; Moore, J. S.; Sottos, N. R. Force-Induced Activation of Covalent Bonds in Mechanoresponsive Polymeric Materials. *Nature* **2009**, *459*, 68−72.

(14) Barbee, M. H.; Kouznetsova, T.; Barrett, S. L.; Gossweiler, G. R.; Lin, Y.; Rastogi, S. K.; Brittain, W. J.; Craig, S. L. Substituent Effects and Mechanism in a Mechanochemical Reaction. *J. Am. Chem. Soc.* **2018**, *140*, 12746−12750.

(15) Chen, Y.; Spiering, A. J. H.; Karthikeyan, S.; Peters, G. W. M.; Meijer, E. W.; Sijbesma, R. P. Mechanically Induced Chemiluminescence from Polymers Incorporating a 1,2-Dioxetane Unit in the Main Chain. *Nat. Chem.* **2012**, *4*, 559−562.

(16) Wang, L.; Zhou, W.; Tang, Q.; Yang, H.; Zhou, Q.; Zhang, X. Rhodamine-Functionalized Mechanochromic and Mechanofluorescent Hydrogels with Enhanced Mechanoresponsive Sensitivity. *Polymers* **2018**, *10*, 994.

(17) Wang, Z.; Ma, Z.; Wang, Y.; Xu, Z.; Luo, Y.; Wei, Y.; Jia, X. A Novel Mechanochromic and Photochromic Polymer Film: When Rhodamine Joins Polyurethane. *Adv. Mater.* **2015**, *27*, 6469−6474.

(18) Kollarigowda, R. H.; Braun, P. V. Direct and Divergent Solid-Phase Synthesis of Azobenzene and Spiropyran Derivatives. *J. Org. Chem.* **2021**, *86*, 4391−4397.

(19) Sommer, M. Substituent Effects Control Spiropyran-Merocyanine Equilibria and Mechanochromic Utility. *Macromol. Rapid Commun.* **2021**, *42*, No. e2000597.

(20) Peterson, G. I.; Larsen, M. B.; Ganter, M. A.; Storti, D. W.; Boydston, A. J. 3d-Printed Mechanochromic Materials. *ACS Appl. Mater. Interfaces* **2015**, *7*, 577−583.

(21) Vidavsky, Y.; Yang, S. J.; Abel, B. A.; Agami, I.; Diesendruck, C. E.; Coates, G. W.; Silberstein, M. N. Enabling Room-Temperature Mechanochromic Activation in a Glassy Polymer: Synthesis and Characterization of Spiropyran Polycarbonate. *J. Am. Chem. Soc.* **2019**, *141*, 10060−10067.

(22) Basu, A.; Wong, J.; Cao, B.; Boechler, N.; Boydston, A. J.; Nelson, A. Mechanoactivation of Color and Autonomous Shape Change in 3d-Printed Ionic Polymer Networks. *ACS Appl. Mater. Interfaces* **2021**, *13*, 19263−19270.

(23) Li, M.; Liu, W.; Zhang, Q.; Zhu, S. Mechanical Force Sensitive Acrylic Latex Coating. *ACS Appl. Mater. Interfaces* **2017**, *9*, 15156−15163.

(24) Jia, Y.; Wang, W.-J.; Li, B.-G.; Zhu, S. Design and Synthesis of Mechano-Responsive Color-Changing Thermoplastic Elastomer Based on Poly(*N*-Butyl Acrylate)-Spiropyran-Polystyrene Comb-Structured Graft Copolymers. *Macromol. Mater. Eng.* **2018**, *303*, 1800154.

(25) Zhang, H.; Chen, Y.; Lin, Y.; Fang, X.; Xu, Y.; Ruan, Y.; Weng, W. Spiropyran as a Mechanochromic Probe in Dual Cross-Linked Elastomers. *Macromolecules* **2014**, *47*, 6783−6790.

(26) Kempe, F.; Brügner, O.; Buchheit, H.; Momm, S. N.; Riehle, F.; Hameury, S.; Walter, M.; Sommer, M. A Simply Synthesized Tough Polyarylene with Transient Mechanochromic Response. *Angew. Chem. Int. Ed.* **2018**, *57*, 997−1000.

(27) Chen, H.; Yang, F.; Chen, Q.; Zheng, J. A Novel Design of Multi-Mechanoresponsive and Mechanically Strong Hydrogels. *Adv. Mater.* **2017**, *29*, 1606900.

(28) Huang, Y.; Huang, S.; Li, Q. Mechanochromic Polymers Based on Mechanophores. *ChemPlusChem.* **2023**, *88*, No. e202300213.

(29) Li, M.; Zhang, Q.; Zhou; Zhu, S. Let Spiropyran Help Polymers Feel Force! *Prog. Polym. Sci.* **2018**, *79*, 26−39.

(30) Beiermann, B. A.; Davis, D. A.; Kramer, S. L. B.; Moore, J. S.; Sottos, N. R.; White, S. R. Environmental Effects on Mechanochemical Activation of Spiropyran in Linear Pmma. *J. Mater. Chem.* **2011**, *21*, 8443.

(31) Degen, C. M.; May, P. A.; Moore, J. S.; White, S. R.; Sottos, N. R. Time-Dependent Mechanochemical Response of Sp-Cross-Linked Pmma. *Macromolecules* **2013**, *46*, 8917−8921.

(32) Grady, M. E.; Beiermann, B. A.; Moore, J. S.; Sottos, N. R. Shockwave Loading of Mechanochemically Active Polymer Coatings. *ACS Appl. Mater. Interfaces* **2014**, *6*, 5350−5355.

(33) Shannahan, L. S.; Lin, Y.; Berry, J. F.; Barbee, M. H.; Fermen-Coker, M.; Craig, S. L. Onset of Mechanochromic Response in the High Strain Rate Uniaxial Compression of Spiropyran Embedded Silicone Elastomers. *Macromol. Rapid Commun.* **2021**, *42*, 2000449.

(34) Lee, C. K.; Beiermann, B. A.; Silberstein, M. N.; Wang, J.; Moore, J. S.; Sottos, N. R.; Braun, P. V. Exploiting Force Sensitive Spiropyrans as Molecular Level Probes. *Macromolecules* **2013**, *46*, 3746−3752.

(35) Beiermann, B. A.; Kramer, S. L. B.; Moore, J. S.; White, S. R.; Sottos, N. R. Role of Mechanophore Orientation in Mechanochemical Reactions. *ACS Macro Lett.* **2012**, *1*, 163−166.

(36) Beiermann, B. A.; Kramer, S. L. B.; May, P. A.; Moore, J. S.; White, S. R.; Sottos, N. R. The Effect of Polymer Chain Alignment and Relaxation on Force-Induced Chemical Reactions in an Elastomer. *Adv. Funct. Mater.* **2014**, *24*, 1529−1537.

(37) Raisch, M.; Genovese, D.; Zaccheroni, N.; Schmidt, S. B.; Focarete, M. L.; Sommer, M.; Gualandi, C. Highly Sensitive, Anisotropic, and Reversible Stress/Strain-Sensors from Mechanochromic Nanofiber Composites. *Adv. Mater.* **2018**, *30*, 1802813.

(38) Kempe, F.; Metzler, L.; Brügner, O.; Buchheit, H.; Walter, M.; Komber, H.; Sommer, M. Substituent-Controlled Energetics and Barriers of Mechanochromic Spiropyran-Functionalized Poly(ε-Caprolactone). *Macromol. Chem. Phys.* **2023**, *224*, 2200254.

(39) Lin, Y.; Barbee, M. H.; Chang, C.-C.; Craig, S. L. Regiochemical Effects on Mechanophore Activation in Bulk Materials. *J. Am. Chem. Soc.* **2018**, *140*, 15969−15975.

(40) Gossweiler, G. R.; Kouznetsova, T. B.; Craig, S. L. Force-Rate Characterization of Two Spiropyran-Based Molecular Force Probes. *J. Am. Chem. Soc.* **2015**, *137*, 6148−6151.

(41) Brügner, O.; Walter, M. Temperature and Loading Rate Dependent Rupture Forces from Universal Paths in Mechanochemistry. *Phys. Rev. Mater.* **2018**, *2*, 113603.

(42) Silberstein, M. N.; Cremar, L. D.; Beiermann, B. A.; Kramer, S. B.; Martinez, T. J.; White, S. R.; Sottos, N. R. Modeling Mechanophore Activation within a Viscous Rubbery Network. *J. Mech. Phys. Solids* **2014**, *63*, 141−153.

(43) Silberstein, M. N.; Min, K.; Cremar, L. D.; Degen, C. M.; Martinez, T. J.; Aluru, N. R.; White, S. R.; Sottos, N. R. Modeling Mechanophore Activation within a Crosslinked Glassy Matrix. *J. Appl. Phys.* **2013**, *114*, 023504.

(44) Tian, W.; Tian, J. An Insight into the Solvent Effect on Photo-, Solvato-Chromism of Spiropyran through the Perspective of Intermolecular Interactions. *Dyes Pigm.* **2014**, *105*, 66−74.

(45) Epstein, E.; Kim, T. A.; Kollarigowda, R. H.; Sottos, N. R.; Braun, P. V. Force-Modulated Equilibria of Mechanophore−Metal Coordinate Bonds. *Chem. Mater.* **2020**, *32*, 3869−3878.

(46) Shiraishi, Y.; Itoh, M.; Hirai, T. Thermal Isomerization of Spiropyran to Merocyanine in Aqueous Media and Its Application to Colorimetric Temperature Indication. *Phys. Chem. Chem. Phys.* **2010**, *12*, 13737.

(47) Wang, J.; Gao, X.; Boarino, A.; Célerse, F.; Corminboeuf, C.; Klok, H.-A. Mechanical Acceleration of Ester Bond Hydrolysis in Polymers. *Macromolecules* **2022**, *55*, 10145−10152.

(48) Wang, J.; Kouznetsova, T. B.; Craig, S. L. Single-Molecule Observation of a Mechanically Activated Cis-to-Trans Cyclopropane Isomerization. *J. Am. Chem. Soc.* **2016**, *138*, 10410−10412.

(49) Hertel, R.; Maftuhin, W.; Walter, M.; Sommer, M. Conformer Ring Flip Enhances Mechanochromic Performance of Ansa -Donor−Acceptor−Donor Mechanochromic Torsional Springs. *J. Am. Chem. Soc.* **2022**, *144*, 21897−21907.

(50) Wu, M.; Li, Y.; Yuan, W.; De Bo, G.; Cao, Y.; Chen, Y. Cooperative and Geometry-Dependent Mechanochromic Reactivity through Aromatic Fusion of Two Rhodamines in Polymers. *J. Am. Chem. Soc.* **2022**, *144*, 17120−17128.

(51) Baumann, C.; Willis-Fox, N.; Campagna, D.; Rognin, E.; Marten, P.; Daly, R.; Göstl, R. Regiochemical Effects for the Mechanochemical Activation of 9-Π-Extended Anthracene-Maleimide Diels−Alderk Adducts. *J. Polym. Sci.* **2022**, *60*, 3128−3133.

(52) Zhang, Y.; Wang, Z.; Kouznetsova, T. B.; Sha, Y.; Xu, E.; Shannahan, L.; Fermen-Coker, M.; Lin, Y.; Tang, C.; Craig, S. L. Distal Conformational Locks on Ferrocene Mechanophores Guide Reaction Pathways for Increased Mechanochemical Reactivity. *Nat. Chem.* **2021**, *13*, 56−62.

(53) Wang, J.; Kouznetsova, T. B.; Kean, Z. S.; Fan, L.; Mar, B. D.; Martinez, T. J.; Craig, S. L. A Remote Stereochemical Lever Arm Effect in Polymer Mechanochemistry. *J. Am. Chem. Soc.* **2014**, *136*, 15162−15165.

(54) Stevenson, R.; De Bo, G. Controlling Reactivity by Geometry in Retro-Diels-Alder Reactions under Tension. *J. Am. Chem. Soc.* **2017**, *139*, 16768−16771.

(55) Wang, Z.; Craig, S. L. Stereochemical Effects on the Mechanochemical Scission of Furan−Maleimide Diels−Alder Adducts. *Chem. Commun.* **2019**, *55*, 12263−12266.

(56) Wang, J.; Kouznetsova, T. B.; Craig, S. L. Reactivity and Mechanism of a Mechanically Activated Anti-Woodward-Hoffmann-Depuy Reaction. *J. Am. Chem. Soc.* **2015**, *137*, 11554−11557.

(57) Akbulatov, S.; Tian, Y.; Huang, Z.; Kucharski, T. J.; Yang, Q. Z.; Boulatov, R. Experimentally Realized Mechanochemistry Distinct from Force-Accelerated Scission of Loaded Bonds. *Science* **2017**, *357*, 299−303.

(58) Bowser, B. H.; Craig, S. L. Empowering Mechanochemistry with Multi-Mechanophore Polymer Architectures. *Polym. Chem.* **2018**, *9*, 3583−3593.

(59) Wu, D.; Lenhardt, J. M.; Black, A. L.; Akhremitchev, B. B.; Craig, S. L. Molecular Stress Relief through a Force-Induced Irreversible Extension in Polymer Contour Length. *J. Am. Chem. Soc.* **2010**, *132*, 15936−15938.

(60) Hodge, P. Entropically Driven Ring-Opening Polymerization of Strainless Organic Macrocycles. *Chem. Rev.* **2014**, *114*, 2278−2312.

(61) Klukovich, H. M.; Kouznetsova, T. B.; Kean, Z. S.; Lenhardt, J. M.; Craig, S. L. A Backbone Lever-Arm Effect Enhances Polymer Mechanochemistry. *Nat. Chem.* **2013**, *5*, 110−114.

(62) Oesterhelt, F.; Rief, M.; Gaub, H. E. Single Molecule Force Spectroscopy by Afm Indicates Helical Structure of Poly(Ethylene-Glycol) in Water. *New J. Phys.* **1999**, *1*, 6−6.

(63) Gossweiler, G. R.; Kouznetsova, T. B.; Craig, S. L. Force-Rate Characterization of Two Spiropyran-Based Molecular Force Probes. *J. Am. Chem. Soc.* **2015**, *137*, 6148−6151.

(64) Barbee, M. H.; Kouznetsova, T.; Barrett, S. L.; Gossweiler, G. R.; Lin, Y.; Rastogi, S. K.; Brittain, W. J.; Craig, S. L. Substituent Effects and Mechanism in a Mechanochemical Reaction. *J. Am. Chem. Soc.* **2018**, *140*, 12746−12750.

(65) Sheng, Y.; Leszczynski, J.; Garcia, A. A.; Rosario, R.; Gust, D.; Springer, J. Comprehensive Theoretical Study of the Conversion Reactions of Spiropyrans: Substituent and Solvent Effects. *J. Phys. Chem. B* **2004**, *108*, 16233−16243.

(66) Keum, S.-R.; Hur, M.-S.; Kazmaier, P. M.; Buncel, E. Thermo- and Photochromic Dyes: Indolino-Benzospiropyrans. Part 1. Uv−Vis Spectroscopic Studies of 1,3,3-Spiro(2 H −1-Benzopyran-2,2′-Indolines) and the Open-Chain Merocyanine Forms; Solvatochromism and Medium Effects on Spiro Ring Formation. *Can. J. Chem.* **1991**, *69*, 1940−1947.

(67) Wojtyk, J. T. C.; Wasey, A.; Kazmaier, P. M.; Hoz, S.; Buncel, E. Thermal Reversion Mechanism of N-Functionalized Merocyanines to Spiropyrans: A Solvatochromic, Solvatokinetic, and Semiempirical Study. *J. Phys. Chem. A* **2000**, *104*, 9046−9055.

(68) Swansburg, S.; Buncel, E.; Lemieux, R. P. Thermal Racemization of Substituted Indolinobenzospiropyrans: Evidence of Competing Polar and Nonpolar Mechanisms. *J. Am. Chem. Soc.* **2000**, *122*, 6594−6600.

(69) Sheng, Y.; Leszczynski, J. Thermal Racemization of Spiropyrans: Implication of Substituent and Solvent Effects Revealed by Computational Study. *Struct. Chem.* **2014**, *25*, 667−677.

(70) Bell, G. I. Models for the Specific Adhesion of Cells to Cells: A Theoretical Framework for Adhesion Mediated by Reversible Bonds between Cell Surface Molecules. *Science* **1978**, *200*, 618−627.

(71) Dudko, O.; Hummer, G.; Szabo, A. Intrinsic Rates and Activation Free Energies from Single-Molecule Pulling Experiments. *Phys. Rev. Lett.* **2006**, *96*, 108101.

(72) Reichardt, C. Empirical Parameters of Solvent Polarity as Linear Free-Energy Relationships. *Angew. Chem. Int. Ed.* **1979**, *18*, 98−110.

(73) Jencks, W. P. A Primer for the Bema Hapothle. An Empirical Approach to the Characterization of Changing Transition-State Structures. *Chem. Rev.* **1985**, *85*, 511−527.

(74) Sun, Y.; Kevlishvili, I.; Kouznetsova, T.; Burke, Z.; Craig, S.; Kulik, H.; Moore, J. The Tension Activated Carbon−Carbon Bond. *ChemRxiv* **2023**.

https://doi.org/10.1021/jacs.3c11621
J. Am. Chem. Soc. 2024, 146, 3920−3925